Scientia Iranica A (2015) 22(2), 345–366

Sharif University of Technology
Scientia Iranica
Transactions A: Civil Engineering
www.scientiairanica.com

Sizing optimization of skeletal structures with a multi-adaptive harmony search algorithm

A. Kaveh[a,*] **and M. Naeimi**[b]

a. *Centre of Excellence for Fundamental Studies in Structural Engineering, Iran University of Science and Technology, Narmak, Tehran, P.O. Box 16846-13114, Iran.*
b. *Faculty of Earthquake Engineering, Road, Housing and Urban Development Research Centre, Tehran, P.O. Box 1464738831, Iran.*

Received 25 June 2013; received in revised form 2 March 2014; accepted 18 November 2014

KEYWORDS
Meta-heuristic algorithms;
Multi-adaptive harmony search;
Harmony search variants;
Size optimization;
Truss optimization;
Frame optimization.

Abstract. The Harmony Search (HS) algorithm is a popular metaheuristic optimization method that reproduces the music improvisation process in searching for a perfect state of harmony. HS has a remarkable ability in detecting near global optima at low computational cost but may be ineffective in performing local search. This study presents the Multi-Adaptive Harmony Search (MAHS) algorithm for sizing optimization of skeletal structures with continuous or discrete design variables. The main difference between the proposed algorithm and classic HS is the way of choosing and adjusting the bandwidth distance (bw). Furthermore, MAHS dynamically updates the Harmony Memory Consideration Rate (HMCR) and Pitch-Adjusting Rate (PAR) parameters during the search process. The robustness and performance of the MAHS algorithm are evaluated in comparison with literature, and in particular, with well-known HS variants such as Global-best Harmony Search (GHS), Self-Adaptive Harmony Search (SAHS), and Efficient Harmony Search (EHS). Optimization results obtained by the MAHS algorithm confirm the validity of the proposed approach.

1. Introduction

Classical optimization techniques (e.g. linear, non-linear, geometric, integer, stochastic, and dynamic programming) may use differential calculus to find the optimum solution. Therefore, these methods could not be efficient in real problems entailing discontinuous, non-convex and non-differentiable cost functions. Moreover, gradient information can be time consuming or even impossible to obtain. These limitations pushed researchers towards developing meta-heuristic optimization methods.

Generally speaking, a meta-heuristic algorithm is an iterative design generation process employing some heuristic criterion to explore and exploit the search space; in particular, learning strategies may be used to find nearly global optimum solutions [1]. Meta-heuristic algorithms are based on the existing laws of nature; for example, Genetic Algorithms (GA) developed by Holland [2] and Goldberg [3] are inspired from the theory of evolution; Tabu Search (TS) developed by Glover [4], Ant Colony Optimization introduced by Dorigo et al. [5], Particle Swarm Optimizer presented by Eberhart and Kennedy [6] attempt to mimic the social behavior of humans or animals. Simulated Annealing proposed by Kirkpatrick [7], Big Bang-Big Crunch proposed by Erol and Eksin [8] and Charged System Search proposed by Kaveh and Talatahari [9] reproduce physical phenomena.

Harmony Search (HS) is a popular meta-heuristic

*. *Corresponding author. Tel.: +98 21 77240104; Fax: +98 21 77240398*
E-mail address: alikaveh@iust.ac.ir (A. Kaveh)

optimization algorithm first introduced by Geem et al. in 2001 [10]. The optimization search reproduces the music improvisation process to find a perfect state of harmony. HS has several excellent features that make it one of the most attractive meta-heuristic algorithms. For example, the very simple formulation makes HS very suited for hybridization with other optimization algorithms. Other features such as easiness and robustness explain why the HS algorithm was applied to different science and engineering optimization problems including computer science (web page clustering, internet routing, robotics), electrical engineering (energy system dispatch, power system design, cell phone network), civil engineering (structural design, water network design, dam scheduling, vehicle routing, groundwater management, flood model calibration), mechanical engineering (heat exchanger design, satellite heat pipe design, offshore structure mooring), biological and biomedical applications (RNA structure prediction, hearing aids, and medical physics) [11].

The original structure of the HS algorithm was often modified to improve its robustness also based on the character of the considered optimization problems. For example, Mahdavi et al. [12] developed an Improved Harmony Search (IHS) where Pitch-Adjusting Rate (PAR) and bandwidth distance (bw) are dynamically adjusted in the search process. Geem [13] proposed a novel stochastic derivative harmony search for discrete design variables. Omran and Mahdavi [14] developed the Global-best Harmony Search (GHS) algorithm. Wang and Huang [15] introduced the Self-Adaptive Harmony Search (SAHS) based on a novel pitch adjusting strategy. Fesanghary et al. [16] utilized the Sequential Quadratic Programming (SQP) as local search tool in the HS search process. Saka and Hasancebi [17] developed the Adaptive Harmony Search (AHS) algorithm which dynamically adjusts HMCR and PAR based on the values taken by these parameters in the optimization process. HS variants are said non-hybridized if the modifications of the original HS formulation regard only the algorithm internal parameters. Conversely, hybridized HS variants combine HS with other optimization algorithms.

This paper presents an improved version of the HS algorithm, named as Multi-Adaptive Harmony Search (MAHS), where HS internal parameters are adaptively modified in the optimization process. The new algorithm is tested in sizing optimization of structures with continuous and discrete design variables.

The remainder of the article is arranged as follows. Section 2 recalls the statement of the design optimization problem for skeletal structures. The classical HS algorithm is described in Section 3. Section 4 describes in detail the Multi-Adaptive Harmony Search algorithm (MAHS) developed in this research. Section 5 presents the results obtained in classical test problems with continuous (planar and spatial truss structures) or discrete optimization variables (planar frames); MAHS results are then compared with literature. Finally, the last section provides some concluding remarks.

2. Weight minimization of skeletal structures

In optimization of structural design, there are three important types of optimal design approaches [18]: (1) Sizing optimization searches for the optimal cross-section size of the elements of a structure with a fixed configuration; (2) Geometric optimization which searches for a set of geometric and cross section size using a given topology; and (3) Topological optimization that selects the best structure from different structural types.

The minimum weight design problem for a skeletal structure can be formulated as follows:

$$\text{Minimize } W(\vec{A}) = \sum_{k=1}^{g} A_k \sum_{i=I}^{mg} \rho_i L_i, \tag{1}$$

where $W(\vec{A})$ is the design vector containing the cross-sectional areas of the elements included as optimization variables $\vec{A} = \{A_1, A_2, ..., A_g\}$, g is the total number of design variables (i.e. number of member groups), A_k is the cross sectional area of the members belonging to group k, mg is the number of members in group k, ρ_i is the material density of member i, L_i is the length of member i.

Truss structures can be subjected to the following optimization constraints:

$$0 \le \sigma \le \sigma_{\max} \quad \text{for tension members,} \tag{2}$$

$$\sigma^b \le \sigma \le 0 \quad \text{for compression members,} \tag{3}$$

$$\delta_{\min} \le \delta_j \le \delta_{\max} \quad \text{for free nodes,} \tag{4}$$

$$A_{\min} \le A_k \le A_{\max} \quad \text{for sizing variables,} \tag{5}$$

where $\sigma_{\max}$ is the allowable stress for tension members, σ^b is the allowable buckling stress for compression member, δ_j is the displacement of the jth node, min and max are the lower and upper bounds for allowable stress, displacement and cross-sectional area.

For frame structures, the AISC specification is used and the LRFD interaction (equations H1-1a, b) [19] for members in flexure and axial compression is defined as:

$$\beta_i = \frac{P_u}{2\phi_c P_n} + \left(\frac{M_{ux}}{\phi_b M_{nx}} + \frac{M_{uy}}{\phi_b M_{ny}}\right) - 1.0 \ge 0$$

$$\text{if} \quad \frac{P_u}{\phi_c P_n} < 0.2, \tag{6}$$

$$\beta_i = \frac{P_u}{\phi_c P_n} + \frac{8}{9}\left(\frac{M_{ux}}{\phi_b M_{nx}} + \frac{M_{uy}}{\phi_b M_{ny}}\right) - 1.0 \geq 0$$

$$\text{if} \quad \frac{P_u}{\phi_c P_n} \geq 0.2, \tag{7}$$

$$\text{Inter-storey drift} < h/300, \tag{8}$$

where P_u is the required axial strength (tension or compression); P_n is the nominal axial strength (tension or compression); ϕ_c is the resistance factor ($\phi_c = 0.9$ for tension, $\phi_c = 0.85$ for compression members); M_{ux} and M_{uy} are the required flexural strengths in the x and y directions, respectively; M_{nx} and M_{ny} are the nominal flexural strengths in the x and y directions (for two-dimensional structures, $M_{ny} = 0$); ϕ_b is the flexural resistance reduction factor ($\phi_b = 0.90$); and h is the story height.

The penalty function is defined as:

$$\beta = \sum_{i=I}^{q} \beta_i, \tag{9}$$

$$f_{\text{penalty}}(\vec{A}) = (1 + \varepsilon_1 \beta)^{\varepsilon_2}, \tag{10}$$

where q is the number of optimization constraints.

In utilizing the penalty function, after analyzing the structure, if the ith constraint is satisfied then β_i will be considered as zero, if not, it will be normalized to the allowable value. The structural weight determined with Eq. (1) is multiplied by the penalty function (10) to form the pseudo-objective function. If all constraints are satisfied, the penalty terms β_i are all set equal to zero and the pseudo-objective function coincides with the structural weight. Conversely, if some constraint is violated, the corresponding penalty term β_i is set equal to the ratio between the constraint value and the allowable constraint limit. Values of parameters ε_1 and ε_2 are selected from sensitivity analysis; in particular, ε_1 is set equal to 1 while ε_2 increases linearly from 1.5 to 3 (see [20] for more details).

3. Classic harmony search

The Harmony Search algorithm reproduces the musical process of searching for a perfect state of harmony. Optimization variables are analogous to musical instruments, values of variables correspond to musical notes and the design vector corresponds to a melody. The optimization process of classical HS includes the following steps [10].

Step 1. Initialization of the HS parameters. By setting HS internal parameters appropriately, it is possible to enhance the performance of the optimization algorithm. The following parameters must be initialized: (i) Harmony Memory Size (HMS) that defines the number of design vectors stored in the Harmony Memory matrix; (ii) Harmony Memory Considering Rate (HMCR) that determines the probability of choosing a new harmony from the Harmony Memory; (iii) the Pitch-Adjusting Rate (PAR) that sets the probability of adjusting values selected from the Harmony Memory.

Step 2. Initialization of Harmony Memory (HM). The Harmony Memory (HM) matrix stores a number of design vectors retained in the optimization process. Because each row of the HM matrix corresponds to a design vector, Harmony Memory is a HMS$\times(N+1)$ matrix. The HM matrix is initialized with randomly generated design vectors that are sorted by the objective function value:

$$\text{HM} = \left[\begin{array}{cccc|c} a_1^1 & a_2^1 & \cdots & a_N^1 & f(A^1) \\ a_1^2 & a_2^2 & \cdots & a_N^2 & f(A^2) \\ \vdots & \vdots & \ddots & \vdots & \vdots \\ a_1^{\text{HMS}} & a_2^{\text{HMS}} & \cdots & a_N^{\text{HMS}} & f(A^{\text{HMS}}) \end{array}\right]. \tag{11}$$

The purpose of using the HM matrix is to retain better designs during the search process.

Step 3. Improvising a new harmony. Each trial design is called a "harmony" and generating a new harmony is called "improvisation". A new harmony $A^{\text{new}} = \{a_1^{\text{new}}; a_2^{\text{new}}; a_3^{\text{new}}; ...; a_{N-1}^{\text{new}}; a_N^{\text{new}}\}$ is generated by following three rules: (1) HM consideration that makes a new harmony to be selected from values stored in HM. Good solutions stored in HM are hence taken into account during the search process; (2) Pitch adjustment refines values selected from HM. This rule makes the algorithm to explore more regions in the neighborhood of the currently selected solution; (3) Random selection from the whole range currently available for each design variable increases the diversity of the solutions and allows local optima trap to be bypassed.

For example, if rule (1) is followed, the value of the first design variable $\{a_1^{\text{new}}\}$ included in the new harmony can be selected from the first column the HM matrix $\{a_1^1; a_1^2; ...; a_1^{\text{HMS}-1}; a_1^{\text{HMS}}\}$. In case some other design variables $\{a_2^{\text{new}}; a_3^{\text{new}}; ...; a_{N-1}^{\text{new}}; a_N^{\text{new}}\}$ are included in this rule, they will be selected in a similar fashion.

The HMCR parameter corresponds to the probability of selecting the new value of a design variable from the previously recorded values stored in the HM matrix. Therefore, (1-HMCR) is the probability of randomly choosing a value from the entire range of available values. For example, HMCR=0.80 means that the HS algorithm will have 80% probability of

choosing the new value of the design variable from the values stored in the HM matrix and only 20% probability of choosing the new value from the entire range of values. Setting HMCR=1.0 is not appropriate because this will raise the risk of getting stuck in a local optimum. The HMCR rule is applied as follows:

$$a_i^{\text{new}} \leftarrow \begin{cases} a_i^{\text{new}} \in \{a_i^1, a_i^2, ..., a_i^{\text{HMS}}\} \\ \quad \text{with probability HMSR} \\ a_i^{\text{new}} \in [A_{\min}, A_{\max}] \\ \quad \text{with probability (1-HMCR)} \end{cases} \tag{12}$$

Every design variable of the new harmony chosen from HM is checked to determine whether it should be modified or not. This procedure uses the PAR parameter that sets the probability of adjusting the values chosen from the HM as follows:

$$\text{pitch adjusting decision for } a_i^{\text{new}} \leftarrow \begin{cases} \text{yes} & \text{with probability PAR} \\ \text{no} & \text{with probability (1-PAR)} \end{cases} \tag{13}$$

The PAR parameter controls the exploitation process in the neighborhood of the solution currently selected from HM. The (1-PAR) term hence represents the probability of leaving the selected value unchanged. The new design variable is adjusted as:

$$a_i^{\text{new}} \leftarrow \begin{cases} a_i^{\text{new}} + \text{rand}[-1,1] \times bw \\ \quad \text{for continuous design variables} \\ a_i^{\text{new}}(k \pm m) \\ \quad \text{for discrete design variables} \end{cases} \tag{14}$$

where bw is an arbitrary distance bandwidth in the case of a continuous variable and rand[-1,1] is a random number uniformly distributed between -1 and 1; k is the current index number. and m is an integer number called neighboring index.

Step 4. Evaluating objective function and updating the harmony memory. If the new harmony $A^{\text{new}} = \{a_1^{\text{new}}; a_2^{\text{new}}; ...; a_N^{\text{new}}\}$ is better than the worst design vector stored in the HM matrix (i.e. A^{HMS}), the new harmony is included in HM to replace the worst harmony. The Harmony Memory is sorted again based on the values of objective function computed for the different trial designs.

Step 5. Terminating the optimization process. The iterative process of Steps 3 and 4 is repeated until the termination criterion is satisfied. In the present study, the algorithm stops when a predefined Number of Improvisations (NI) is reached; NI corresponds the number of objective function evaluations. The best design vector stored in the HM is finally taken as the optimum design.

4. Multi-adaptive harmony search

Classic Harmony Search can find nearly global optima rather quickly. However, since parameters HMCR, PAR and bw are kept constant throughout the search process, its local search is relatively inefficient. The MAHS algorithm developed in this research includes the same steps as classical HS except for Step 3 where the HMCR and PAR parameters are dynamically updated and two different formulations are applied to update the bandwidth parameter bw.

4.1. Continuous design variables

4.1.1. Update of the bandwidth parameter

The bandwidth parameter (bw) serves for pitch-adjusting continuous design variables. Large values of bw should be used in the early optimization iterations to explore large regions of the design space thus approaching the global optimum. Conversely, small values of bw should be used in the final optimization cycles where exploitation capability is required for performing efficient local search. In order to balance diversification in initial search steps and intensification in the final search steps, bw must dynamically change during the search process. For that purpose, MAHS sets the bw parameter as:

$$bw(\text{NI}) = bw_{\min} - (bw_{\min} - bw_{\max}) \times \left(1 - \frac{\text{NI}}{\max \text{NI}}\right)^2$$
$$\text{with probability } P_{bw}, \tag{15}$$

$$bw(\text{NI}) = [\max(\text{HM}_i) - \min(\text{HM}_i)]$$
$$\text{with probability } (1 - P_{bw}), \tag{16}$$

where $bw_{\max}$ and $bw_{\min}$ are the maximum and minimum bandwidth values, respectively; NI denotes the current improvisation (i.e. number of structural analyses); maxNI is the maximum number of improvisations; bw(NI) is the bandwidth distance used in the NIth improvisation; min(HM_i) and max(HM_i), respectively, are the minimum and maximum values of the ith design variable stored in the HM matrix.

The value of bw determined from Eq. (15) decreases quadratically with the number of improvisations. Using quadratic variation will raise the reduction rate of the bw parameter relative to linear variation. This causes the bw parameter to approach faster to its minimum value ($bw_{\min}$). By using this strategy, exploitation capability required for performing efficient local search can be improved. In the early optimization cycles, HS explores large regions of design space

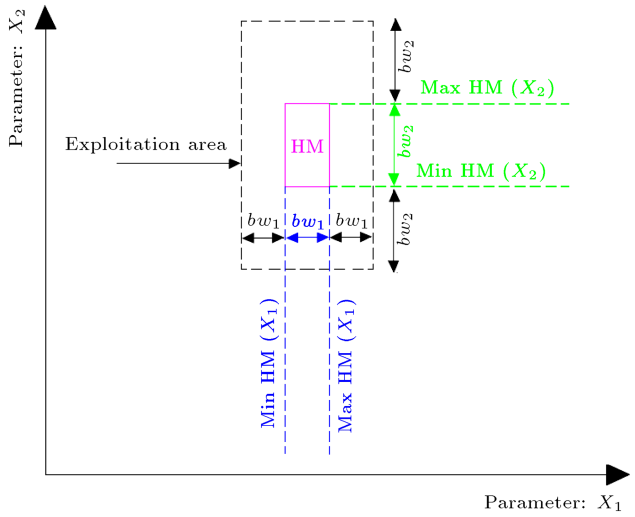

Figure 1. Illustration of the use of Eq. (16).

because the [max(HM_i)-min(HM_i)] difference is large. Thus, MAHS concentrates more on diversification. As the minimum and maximum values of the ith design variable stored in HM eventually approach the optimum, the [max(HM_i)-min(HM_i)] difference tends to become zero. Therefore, the optimization algorithm focuses more on intensification.

A new design vector is generated in the neighborhood of the harmony memory with Eq. (16); consequently, MAHS approaches quickly the region of design space containing the global optimum. Figure 1 illustrates this process for a 2D optimization problem. Besides values included in the HM matrix, neighboring values can be considered in the formation of the new solution.

If the pitch-adjusted value, a_i^{new}, violates side constraints, the value of the ith design variable is reset as follows:

$$a_i^{\text{new}} \leftarrow a_i^{\min} + \text{rand} \times (a_i^{\text{old}} - a_i^{\min})$$

$$\text{if} \quad a_i^{\text{new}} \le a_i^{\min}, \tag{17}$$

$$a_i^{\text{new}} \leftarrow a_i^{\max} - \text{rand} \times (a_i^{\max} - a_i^{\text{old}})$$

$$\text{if} \quad a_i^{\text{new}} \ge a_i^{\max}, \tag{18}$$

where a_i^{old} is the value of the ith design variable before pitch-adjusting; $a_i^{\min}$ and $a_i^{\max}$, respectively, are the corresponding side constraints.

4.1.2. Update of the new P_{bw} parameter

As the difference of [max(HM_i)-min(HM_i)] approaches zero in the final search steps, the probability of choosing Eq. (16) should decrease. For that purpose, MAHS utilizes the new parameter P_{bw} to choose the equation for updating bw. In particular, P_{bw} is dynamically updated during the search process as:

$$P_{bw}(\text{NI}) = P_{bw,\min} + \frac{P_{bw,\max} - P_{bw,\min}}{\text{Max NI}} \times \text{NI}. \tag{19}$$

It appears that P_{bw} increases linearly in the optimization process. A random number uniformly distributed in the interval (0,1) is generated. If this random number is smaller than P_{bw}, the value of bw is chosen from Eq. (15), otherwise Eq. (16) is utilized. Therefore, MAHS is more likely to use Eq. (16) for updating bw in the initial iterations. Conversely, because P_{bw} gradually increases towards the end optimization process, where Eq. (16) approaches zero, choosing Eq. (15) to update bw is more probable.

4.1.3. Update of the HMCR parameter

The HMCR and PAR parameters are used to improve the current solution. Unlike classic HS, the harmony memory considering rate parameter is dynamically updated in MAHS as:

$$\text{HMCR(NI)} = \text{HMCR}_{\min} + (\text{HMCR}_{\max} - \text{HMCR}_{\min}) \times \left(\frac{\text{NI}}{\text{Max NI}}\right)^{0.1}. \tag{20}$$

This causes the probability of choosing one value from historical values stored in the harmony memory to increase during the search process. The exponent 0.1 for Eq. (20), causes the value of HMCR to increase faster in the early optimization iterations. In other words, in the final search steps, the new design variable is selected almost from the values stored in HM. This can enhance intensification in the final search steps. The typical variation of HMCR versus the number of improvisations is shown in Figure 2.

4.1.4. Update of the PAR parameter

The pitch adjusting rate parameter, also, is dynamically updated in the search process. In particular, it decreases with the number of improvisations:

$$\text{PAR(NI)} = \text{PAR}_{\max} - (\text{PAR}_{\max} - \text{PAR}_{\min}) \times \left(\frac{\text{NI}}{\text{Max NI}}\right)^{2}. \tag{21}$$

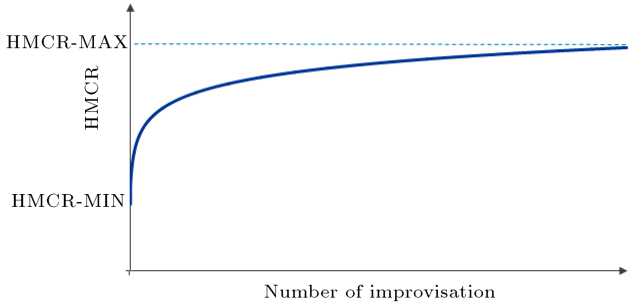

Figure 2. Typical variation of HMCR with the number of improvisation.

By setting PAR to a large value, it is possible to increase the probability of pitch-adjusting the values selected from HM. This enhances the diversification ability of MAHS in the initial iterations. The PAR parameter reduces to its minimum value in the final iterations, enough for performing local search that focuses more on intensification. By using this quadratic variation, the reduction rate of the PAR parameter increases in final stage of search.

4.2. Discrete design variables

For optimization problems with discrete design variables, P_{bw}, PAR, HMCR parameters are defined as in Section 4.1 with only a difference: the bandwidth bw is replaced by the neighboring index m, which is an integer number:

$$m(\mathrm{NI}) = \mathrm{Ceil}\left\langle m_{\min} - (m_{\min} - m_{\max}) \times \left(1 - \frac{\mathrm{NI}}{\mathrm{Max\ NI}}\right)^2 \right\rangle \quad \text{with probability } P_{bw}, \tag{22}$$

$$m(\mathrm{NI}) = [k_{\max}(\mathrm{HM}_i) - k_{\min}(\mathrm{HM}_i)] \quad \text{with probability } (1 - P_{bw}), \tag{23}$$

where $m_{\max}$ and $m_{\min}$ are the maximum and minimum neighboring index values, respectively; $m(\mathrm{NI})$ is neighboring index in the NIth improvisation; "Ceil" is a function that is rounded up to the next highest integer; $k_{\min}(\mathrm{HM}_i)$ and $k_{\max}(\mathrm{HM}_i)$ are the bounds of the ith discrete variable stored in the harmony memory.

If the pitch adjusted value violates side constraints, the value of optimization variable is reset with Eqs. (17) and (18) where $a_i^{\min}$ and $a_i^{\max}$ are replaced by the corresponding discrete variable bounds.

5. Test problems and optimization results

The new multi-adaptive harmony search algorithm developed in this research was tested in classical sizing optimization problems of trusses and frames. Optimum designs obtained by MAHS were compared in detail with other metaheuristic algorithms presented in literature. Furthermore, convergence behavior of MAHS was compared with the Global-Best Harmony Search (GHS) developed by Omran and Mahdavi [14], Self-Adaptive Harmony Search developed by Wang and Huang [15] and used by Degertekin [21], and Efficient Harmony Search, which is originally Improved Harmony Search, was presented by Mahdavi et al. [12] applied by Degertekin [21]. The best combination of internal parameters was determined by sensitivity analysis: $\mathrm{PAR}_{\min} = 0.2 \sim 0.3$, $\mathrm{PAR}_{\max} = 0.7 \sim 0.8$, $\mathrm{HMCR}_{\min}$=0.9, $\mathrm{HMCR}_{\max}$=0.95∼1.0, $P_{bw,\min} = 0.2$ and $P_{bw,\max} = 0.8 \sim 1.0$, HMS=10 ∼ 20, $m_{\min} = 1$ and $m_{\max} = 15$.

In this paper, the parameters of the algorithms are not set initially. In all examples, sensitivity analyses are performed in order to find an appropriate set of parameters to obtain the best result. In sensitivity analysis we fix all parameters except one and we study the variation of that particular parameter. We do this for other parameters to obtain the best combination of parameters; however it is not required to do this for all examples since the parameters set is almost the same in all the examples. Generally, in all examples, the parameters set is considered as follows: $\mathrm{PAR}_{\min}$=0.2∼0.3, $\mathrm{PAR}_{\max}$=0.7∼0.8, $\mathrm{HMCR}_{\min}$=0.9, $\mathrm{HMCR}_{\max}$=0.95∼1.0, $P_{bw,\min}$=0.2 and $P_{bw,\max}$=0.8∼1.0, HMS=10∼20, $m_{\min} = 1$ and $m_{\max} = 15$.

5.1. Truss structures

5.1.1. Planar 10-bar truss

The first test problem is the weight minimization of the planar 10-bar planar shown in Figure 3. The modulus of elasticity of the material is 10 Msi and material density is 0.1 lb/in^3. The maximum stress for all members was set as 25 ksi. The maximum allowable displacement for all free nodes in X and Y directions is set as 2.0 in. The cross-sectional area of each element was included as design variable; therefore, there are 10 sizing variables. The minimum cross-sectional area of all members is 0.1 in^2.

Two different loading cases are considered. In Case 1, concentrated loads of 100 kips are applied at nodes 2 and 4 in the negative Y direction (i.e. $P_1 = 100$ kips and $P_2 = 0$). In Case 2, $P_1 = 150$ kips and $P_2 = 50$ kips hold.

In order to evaluate the sensitivity of the MAHS algorithm to internal parameters, different combinations of internal parameters were considered and independent optimization runs were carried for each combination starting from different initial populations. Table 1 shows the results of the sensitivity analysis performed for Case 1. Once the best combination of

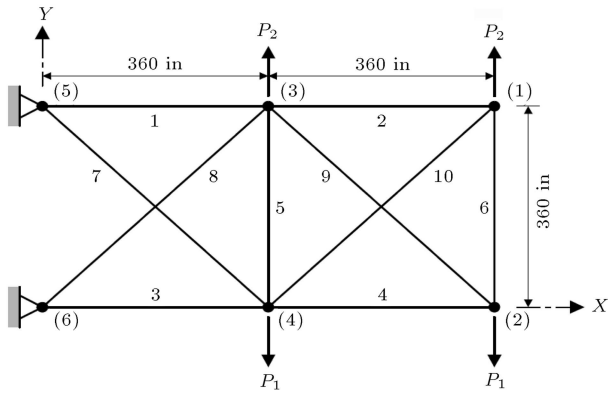

Figure 3. Schematic of the planar 10-bar truss [18].

Table 1. Sensitivity analysis to find the best set of parameters of MAHS for the 10-bar truss (Case 1).

Case	$Pbw_{\min}$	$Pbw_{\max}$	HMS	$HMCR_{\min}$	$HMCR_{\max}$	$PAR_{\min}$	$PAR_{\max}$	$bw_{\min}$	$bw_{\max}$	Average weight (lb)	Best weight (lb)
1	0.2	1	10	0.9	0.95	0.1	0.8	0.1	1	5063.93	5062.77
2	0.2	1	10	0.9	0.95	0.1	0.8	0.01	0.1	5070.49	5061.48
3	0.2	1	10	0.9	0.95	0.1	0.8	0.001	0.01	5073.17	5063.11
4	0.2	1	10	0.9	0.95	0.2	0.8	0.1	1	5064.47	5063.00
5	0.2	1	10	0.9	0.95	0.2	0.8	0.01	0.1	5067.13	5061.65
6	0.2	1	10	0.9	0.95	0.2	0.8	0.001	0.01	5067.41	5063.08
7	0.2	1	10	0.9	0.95	0.3	0.8	0.01	0.1	5062.94	5061.89
8	0.2	1	10	0.9	0.95	0.3	0.8	0.001	0.01	5065.53	5062.05
9	0.2	1	10	0.9	0.95	0.2	0.7	0.01	0.1	5068.70	5061.97
10	0.2	1	10	0.9	0.95	0.2	0.7	0.001	0.01	5066.94	5062.75
11	0.2	1	10	0.9	0.95	0.3	0.7	0.01	0.1	5062.40	5061.55
12	0.2	1	10	0.9	0.95	0.3	0.7	0.001	0.01	5073.23	5063.68
13	0.2	1	10	0.9	1	0.3	0.8	0.01	0.1	5061.81	5061.21
14	0.2	1	10	0.9	1	0.3	0.8	0.001	0.01	5062.18	5061.29
15	0.2	1	10	0.9	1	0.1	0.7	0.01	0.1	5067.94	5061.26
16	0.2	1	10	0.9	1	0.1	0.7	0.001	0.01	5061.53	5061.01
17	0.2	1	10	0.9	1	0.2	0.7	0.01	0.1	5062.47	5061.16
18	0.2	1	10	0.9	1	0.2	0.7	0.001	0.01	5062.18	5060.94
19	0.2	1	10	0.9	1	0.3	0.8	0.01	0.1	5062.28	5061.40
20	0.2	1	10	0.9	1	0.3	0.8	0.001	0.01	5061.78	5061.16
21	0.2	1	20	0.9	1	0.3	0.8	0.01	0.1	5067.85	5063.36
22	0.2	1	20	0.9	1	0.3	0.8	0.001	0.01	5064.26	5061.83
23	0.2	1	20	0.9	1	0.3	0.8	0.001	0.01	5063.52	5061.58
24	0	1	10	0.9	1	0.3	0.8	0.001	0.01	5062.90	5061.31
25	0.1	0.9	10	0.9	1	0.3	0.8	0.001	0.01	5061.99	5061.96
26	0.2	0.8	10	0.9	1	0.3	0.8	0.001	0.01	5061.36	5060.84
27	0.5	1	10	0.9	1	0.3	0.8	0.001	0.01	5067.70	5061.77
28	0.2	0.8	10	0.9	1	0.3	0.8	0.0001	0.001	5064.76	5062.40

internal parameters was determined, 30 independent optimization runs were carried out starting from different initial populations. The maximum number of improvisations was always set equal to 10,000.

Tables 2 and 3 compare the optimization results obtained by MAHS with literature for Case 1 and Case 2, respectively. Statistical data such as the average weight and standard deviation of weight determined for 30 independent optimization runs are included in the table and the best and worst optimized weights obtained in the 30 optimization runs are also shown.

It can be seen that the present algorithm always converges to the best design without violating any optimization constraint. Furthermore, the worst design obtained in the 30 independent optimization runs was just slightly different from the optimized designs reported in literature. Standard deviation on optimized weight was smaller than that found for the SAHS used by Degertekin [21]. This proves that in spite of its stochastic nature, MAHS was always able to correctly converge to the global optimum.

The best designs were obtained after only 8751 and 8325 structural analyses for Case 1 and Case 2, respectively. In Case 1, classic HS obtained the optimum design after 20,000 structural analyses while in Case 2, classic HS required 15,000 structural analyses. However, the SAHS utilized by Degertekin [21] required less structural analyses than MAHS; i.e., respectively, 7081 and 7267 vs. 8751 and 8325.

Converges behavior of MAHS is compared with other HS variants in Figure 4 for Case 1. The maximum number of structural analyses (i.e. number of improvisation) was always set equal to 10,000 for all HS variants.

Table 2. Optimization results obtained for Case 1 of the planar 10-bar truss problem.

Design variables (A_i)	Area (in^2)									
	Lee and Geem [18]	Li et al. [22]			Kaveh and Talatahari [23]	Lamberti and Pappalettere [24]	Degertekin [21]		Present work	
	HS	PSO	PSOPC	HPSO	HPSOACO	IHS	EHS	SAHS	Worst result	Best result
A_1	30.15	33.469	30.569	30.704	30.307	30.5222	30.208	30.394	30.341	30.508
A_2	0.102	0.11	0.1	0.1	0.1	0.1	0.1	0.1	0.1	0.1
A_3	22.71	23.177	22.974	23.167	23.434	23.2005	22.698	23.0 98	22.698	23.155
A_4	15.27	15.475	15.148	15.183	15.505	15.2232	15.275	15.491	15.4	15.31
A_5	0.102	3.649	0.1	0.1	0.1	0.1	0.1	0.1	0.1	0.1
A_6	0.544	0.116	0.547	0.551	0.5241	0.5513	0.529	0.529	0.559	0.552
A_7	7.541	8.328	7.493	7.46	7.4365	7.4572	7.558	7.488	7.55	7.457
A_8	21.56	23.34	21.159	20.978	21.079	21.0367	21.559	21.189	21.509	21.015
A_9	21.45	23.014	21.556	21.508	21.229	21.5288	21.491	21.342	21.339	21.53
A_{10}	0.1	0.19	0.1	0.1	0.1	0.1	0.1	0.1	0.1	0.1
Weight (lb)	5057.88	5529.5	5061	5060.92	5056.56	5060.82	5062.39	5061.42	5062.06	5060.87
Average weight (lb)	N/A	N/A	N/A	N/A	N/A	N/A	5063.73	5061.95	5061.262	
Standard deviation (lb)	N/A	N/A	N/A	N/A	N/A	N/A	1.98	0.71	0.283	
Number of structural analyses	20,000	150,000	150,000	150 ,000	10,650	1,350	9,791	7,081	9,353	8,751

Note : 1 lb=4.45 N; 1 in^2 =6.452 cm^2; N/A : Not Available.

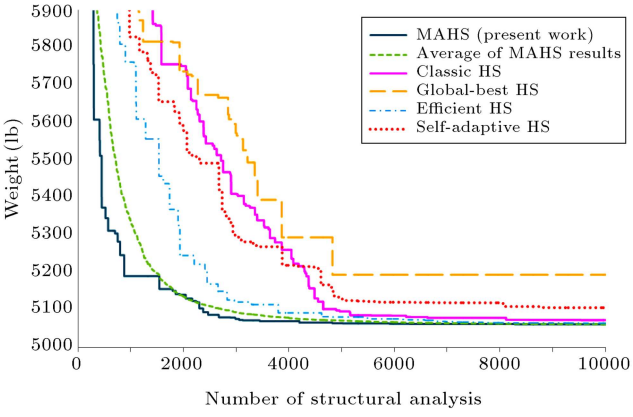

Figure 4. Comparison of HS variants convergence curves obtained for Case 1 of the planar 10-bar truss problem.

It can be seen that the average optimization history of MAHS is very close to the best run. The convergence speed of MAHS was definitely higher than for the other HS variants. EHS outperformed classical HS while GHS was, by far, the worst HS-based optimizer.

5.1.2. Spatial 25- bar truss

The third test problem solved in this study was the weight minimization of the spatial 25-bar truss shown in Figure 5. The modulus of elasticity of the material is 10 Msi while material density is 0.1 lb/in^3. Because of structural symmetry about the X and Y axes, truss elements were grouped into 8 independent groups (i.e. there are 8 sizing design variables) as: (1) A_1, (2) $A_2 \sim A_5$, (3) $A_6 \sim A_9$, (4) $A_{10} \sim A_{11}$, (5) $A_{12} \sim A_{13}$, (6) $A_{14} \sim A_{17}$, (7) $A_{18} \sim A_{21}$, and (8) $A_{22} \sim A_{25}$.

Stress limits in tension and compression for each element group are listed in Table 4. The maximum allowable displacement in every direction for all free nodes is 0.35 in. Cross-sectional areas of all elements must be less than 0.01 in^2. The structure is subject to two independent loading conditions described in Table 5.

Results of sensitivity analysis carried out for finding the best combination of internal parameters are presented in Table 6; five independent runs were performed for each set of parameters. The table reports the best and average structural weights obtained by

Table 3. Optimization results obtained for Case 2 of the planar 10-bar truss problem.

Design variables (A_i)	Area (in^2)										
	Schmit and Farshi [25]	Lee and Geem [18]	Li et al. [22]			Kaveh and Talatahari [23]	Fesanghary and Mahdavi [16]	Degertekin [21]		Present work	
		HS	PSO	PSOPC	HPSO	HPSOACO	SQPHS	EHS	SAHS	Worst result	Best result
A_1	24.29	23.25	22.935	23.743	23.353	23.194	23.31	23.589	23.525	23.469	23.131
A_2	0.1	0.102	0.113	0.101	0.1	0.1	0.1	0.1	0.1	0.1	0.1
A_3	23.35	25.73	25.355	25.287	25.502	24.585	24.63	25.422	25.429	25.734	25.385
A_4	13.66	14.51	14.373	14.413	14.25	14.221	14.59	14.488	14.488	14.031	14.338
A_5	0.1	0.1	0.1	0.1	0.1	0.1	0.1	0.1	0.1	0.1	0.1
A_6	1.969	1.977	1.99	1.969	1.972	1.969	1.967	1.975	1.992	1.971	1.97
A_7	12.67	12.21	12.346	12.362	12.363	12.489	12.49	12.362	12.352	12.46	12.438
A_8	12.54	12.61	12.923	12.694	12.984	12.925	12.94	12.682	12.698	13.24	13.138
A_9	21.97	20.36	20.678	20.323	20.356	20.952	20.51	20.322	20.341	19.853	20.224
A_{10}	0.1	0.1	0.1	0.103	0.101	0.101	0.1	0.1	0.1	0.1	0.1
Weight (lb)	4691.84	4668.81	4679.47	4677.7	4677.29	4675.78	4 668.72	4679.02	4678.84	4678.85	4677.71
Average weight (lb)	N/A	N/A	N/A	N/A	N/A	N/A	N/A	4681.61	4680.08	4678.8	
Standard deviation (lb)	N/A	N/A	N/A	N/A	N/A	N/A	N/A	2.51	1.89	0.407	
Number of structural analyses	N/A	15,000	150,000	150,000	150,000	9,925	22,000	11,402	7,267	9,425	8,325

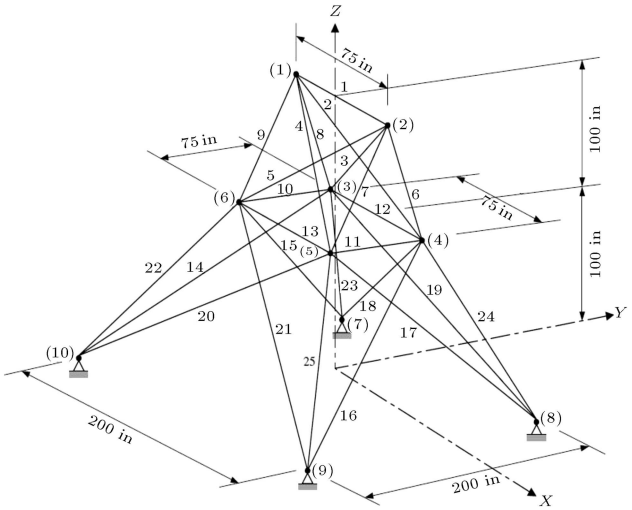

Figure 5. Schematic of the spatial twenty-five-bar truss [18].

Table 4. Stress limits for the spatial 25-bar truss members.

Design variables (A_i)	Allowable compressive stress (ksi)	Allowable tensile stress (ksi)
A_1	35.092	40
A_2-A_5	11.59	40
A_6-A_9	17.305	40
A_{10}-A_{11}	35.092	40
A_{12}-A_{13}	35.092	40
A_{14}-A_{17}	6.759	40
A_{18}-A_{21}	6.959	40
A_{22}-A_{25}	11.082	40

MAHS. In all cases, the maximum number of improvisations (i.e. structural analysis) was set equal to 10,000.

Table 7 compares the optimization results obtained by MAHS with literature. The SAHS algorithm used by Degertekin [21] obtains to the best design overall while the IHS algorithm developed by Lamberti and Pappalettere [24] is the fastest optimizer overall. The optimum design reported for classical HS [18] violated slightly the optimization constraints. Remarkably, the worst result found in the 30 independent runs carried out for MAHS was practically the same as the best design found by the other optimization

algorithms. Similar to the previous examples, the standard deviation on optimized weight found by MAHS was quite small. Classical HS obtained the optimum solution after 15,000 structural analyses while MAHS required only 7,484 structural analyses to complete the optimization process.

Convergence curves presented in Figure 6 confirm that MAHS has a better convergence behavior than other HS variants which rank as in the previous two test cases.

Table 5. Loading conditions for the spatial 25-bar truss (kips).

Node	Condition 1			Condition 2		
	F_x	F_y	F_z	F_x	F_y	F_z
1	0	20	-5	1	10	-5
2	0	-20	-5	0	10	-5
3	0	0	0	0.5	0	0
6	0	0	0	0.5	0	0

5.1.3. Spatial 72-bar truss

In the fourth test problem, the weight of the spatial 72-bar truss shown in Figure 7 is minimized. The modulus of elasticity of the material is 10 Msi and material density is 0.1 lb/in^3. The cross-sectional areas of the

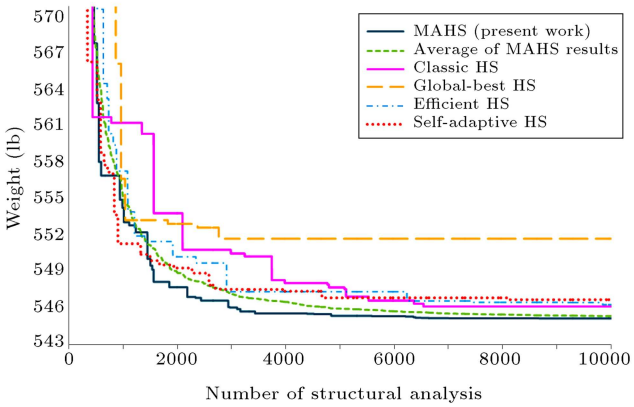

Figure 6. Comparison of HS variants convergence curves obtained for the spatial 25-bar truss problem.

Table 6. Results of sensitivity analysis carried for tuning the MAHS internal parameters for spatial 25-bar truss problem.

Case	Pbw_{min}	Pbw_{max}	HMS	$HMCR_{min}$	$HMCR_{max}$	PAR_{min}	PAR_{max}	bw_{min}	bw_{max}	Average weight (lb)	Best weight (lb)
1	0.2	1	10	0.9	0.95	0.1	0.8	0.1	1	548.15	547.80
2	0.2	1	10	0.9	0.95	0.1	0.8	0.01	0.1	545.35	54524
3	0.2	1	10	0.9	0.95	0.1	0.8	0.001	0.01	545.64	545.19
4	0.2	1	10	0.9	0.95	0.2	0.8	0.1	1	547.11	546.57
5	0.2	1	10	0.9	0.95	0.2	0.8	0.01	0.1	545.44	545.25
6	0.2	1	10	0.9	0.95	0.2	0.8	0.001	0.01	545.41	545.24
7	0.2	1	10	0.9	0.95	0.3	0.8	0.01	0.1	545.39	545.29
8	0.2	1	10	0.9	0.95	0.3	0.8	0.001	0.01	545.76	545.20
9	0.2	1	10	0.9	0.95	0.2	0.7	0.01	0.1	545.56	545.31
10	0.2	1	10	0.9	0.95	0.2	0.7	0.001	0.01	545.85	545.28
11	0.2	1	10	0.9	0.95	0.3	0.7	0.01	0.1	546.41	546.28
12	0.2	1	10	0.9	0.95	0.3	0.7	0.001	0.01	546.07	546.26
13	0.2	1	10	0.9	1	0.3	0.8	0.01	0.1	548.42	547.24
14	0.2	1	10	0.9	1	0.3	0.8	0.001	0.01	545.87	545.19
15	0.2	1	10	0.9	1	0.1	0.7	0.01	0.1	545.63	545.29
16	0.2	1	10	0.9	1	0.1	0.7	0.001	0.01	547.12	545.22
17	0.2	1	10	0.9	1	0.2	0.7	0.01	0.1	546.91	546.29
18	0.2	1	10	0.9	1	0.2	0.7	0.001	0.01	545.64	545.20
19	0.2	1	10	0.9	1	0.3	0.8	0.01	0.1	545.46	545.26
20	0.2	1	10	0.9	1	0.3	0.8	0.001	0.01	545.23	545.17
21	0.2	1	20	0.9	1	0.3	0.8	0.01	0.1	546.55	545.29
22	0.2	1	20	0.9	1	0.3	0.8	0.001	0.01	546.06	545.29
23	0.2	1	20	0.9	1	0.3	0.8	0.001	0.01	546.15	545.48
24	0	1	10	0.9	1	0.3	0.8	0.001	0.01	545.41	545.21
25	0.1	0.9	10	0.9	1	0.3	0.8	0.001	0.01	545.41	545.31
26	0.2	0.8	10	0.9	1	0.3	0.8	0.001	0.01	545.89	545.35
27	0.5	1	10	0.9	1	0.3	0.8	0.001	0.01	549.82	545.51
28	0.2	0.8	10	0.9	1	0.3	0.8	0.0001	0.001	545.87	545.36

Table 7. Optimization results obtained for the planar 25-bar truss problem.

Design variables	Element group	Area (in^2)										
		Lee and Geem [18]	Li et al. [22]			Camp [27]	Lamberti and Pappalettere [24]	Kaveh and Talatahar [28]	Degertekin [21]		Present work	
		HS	PSO	PSOPC	HPSO	BB-BC	IHS	HBB-BC	EHS	SAHS	Worst result	Best result
1	A_1	0.047	9.863	0.01	0.01	0.01	0.01	0.01	0.01	0.01	0.01	0.01
2	A_2-A_5	2.022	1.798	1.979	1.97	2.092	1.9871	1.993	1.995	2.074	1.9217	1.9843
3	A_6-A_9	2.950	3.654	3.011	3.016	2.964	2.9935	3.056	2.98	2.961	3.0885	2.998
4	A_{10}-A_{11}	0.01	0.1	0.1	0.01	0.01	0.01	0.01	0.01	0.01	0.01	0.01
5	A_12-A_{13}	0.014	0.1	0.1	0.01	0.01	0.01	0.01	0.01	0.01	0.01	0.01
6	A_{14}-A_{17}	0.688	0.596	0.657	0.694	0.689	0.6839	0.665	0.696	0.691	0.6768	0.6819
7	A_{18}-A_{21}	1.657	1.659	1.678	1.681	1.601	1.6769	1.642	1.679	1.617	1.6916	1.6773
8	A_{22}-A_{25}	2.663	2.612	2.693	2.643	2.686	2.6622	2.679	2.652	2.674	2.6425	2.6635
Weight (lb)		544.38	627.08	545.27	545.19	545.38	545.15	545.16	545.49	545.12	545.309	545.165
Average weight (lb)		N/A	N/A	N/A	N/A	545.78	N/A	545.66	546.52	545.94	545.236	
Standard deviation (lb)		N/A	N/A	N/A	N/A	0.491	N/A	0.367	1.05	0.91	0.06	
Number of structural analyses		15,000	150,000	50,000	2,500	20,566	1,050	12,500	10, 391	9,051	8,542	7,484

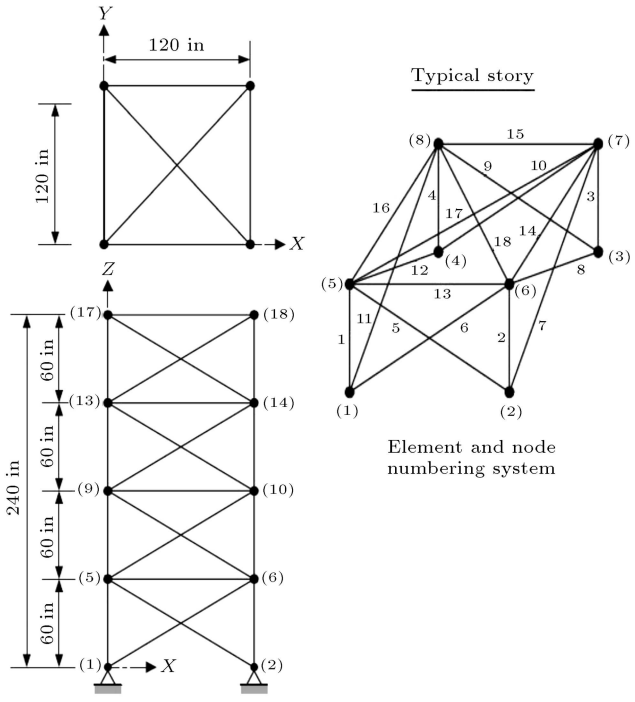

Figure 7. Schematic of the spatial seventy-two-bar truss [18].

72 elements, taken as sizing variables, are divided into 16 groups, because of the structural symmetry about X and Y axes, as follows:

(1) $A_1 \sim A_4$, (2) $A_5 \sim A_{12}$,

(3) $A_{13} \sim A_{16}$, (4) $A_{17} \sim A_{18}$,

(5) $A_{19} \sim A_{22}$, (6) $A_{23} \sim A_{30}$,

(7) $A_{31} \sim A_{34}$, (8) $A_{35} \sim A_{36}$,

(9) $A_{37} \sim A_{40}$, (10) $A_{41} \sim A_{48}$,

(11) $A_{49} \sim A_{52}$, (12) $A_{53} \sim A_{54}$,

(13) $A_{55} \sim A_{58}$, (14) $A_{59} \sim A_{66}$,

(15) $A_{67} \sim A_{70}$, (16) $A_{71} \sim A_{72}$.

Therefore, the test problem has 16 design variables. This spatial truss is subject to two independent loading conditions shown in Table 8. The maximum stress for all members is 25,000 psi. The maximum displacement

of all free nodes in X and Y directions must be less than 0.25 in.

Two problem variants were considered. In Case 1, the minimum cross-sectional area of all members is 0.1 in^2. In Case 2, the minimum cross-sectional area of all members is 0.01 in^2. Tables 9 and 10 report the optimization results and compare MAHS with literature. It can be seen from Table 9 that MAHS obtained the best feasible design. Remarkably, the worst result obtained in the 30 independent runs practically coincides with the optimized weights reported in literature.

Table 10 shows that MAHS found the second best design, very close to that found by Lamberti with efficient simulated annealing [29]. Similar to previous examples, standard deviation on optimized weight was very small. In Case 1, classical HS required 20,000 structural analyses while MAHS converged to the optimum design within only 13,499 analyses. In Case 2, classical HS required 20,000 structural analyses while MAHS required only 12,298 analyses.

Convergence curves of HS variants are shown in

Table 8. Loading conditions for the 72-bar spatial truss (kips).

Node	Condition 1			Condition 2		
	F_x	F_y	F_z	F_x	F_y	F_z
17	5	5	-5	0	0	-5
18	0	0	0	0	0	-5
19	0	0	0	0	0	-5
20	0	0	0	0	0	-5

Table 9. Optimization results obtained for Case 1 of the spatial 72-bar truss problem.

Design variables (A_i)	Element group	Area (in^2)										
		Lee and Geem [18]	Li et al. [22]			Perez and Behdinan [26]	Camp [27]	Kaveh and Talatahar [28]	Degertekin [21]		Present work	
		HS	PSO	PSOPC	HPSO	PSO	BB-BC	HBB-BC	EHS	SAHS	Worst result	Best result
1	A_1-A_4	1.79	41.794	1.855	1.857	1.7427	1.8577	1.9042	1.967	1.86	1.8751	1.8837
2	A_5-A_{12}	0.521	0.195	0.504	0.505	0.5185	0.5059	0.5162	0.51	0.521	0.5176	0.5089
3	A_{13}-A_{16}	0.1	10.797	0.1	0.1	0.1	0.1	0.1	0.1	0.1	0.1	0.1
4	A_{17}-A_{18}	0.1	6.861	0.1	0.1	0.1	0.1	0.1	0.1	0.1	0.1	0.1
5	A_{19}-A_{22}	1.229	0.438	1.253	1.255	1.3079	1.2476	1.2582	1.293	1.271	1.2204	1.26 76
6	A_{23}-A_{30}	0.522	0.286	0.505	0.503	0.5193	0.5269	0.5035	0.511	0.509	0.5096	0.51
7	A_{31}-A_{34}	0.1	18.309	0.1	0.1	0.1	0.1	0.1	0.1	0.1	0.1017	0.1
8	A_{35}-A_{36}	0.1	1.22	0.1	0.1	0.1	0.1012	0.1	0.1	0.1	0.1006	0.1
9	A_{37}-A_{40}	0.517	5.933	0.497	0.496	0.5142	0.5209	0.5178	0.499	0.485	0.5341	0.5286
10	A_{41}-A_{48}	0.504	19.545	0.508	0.506	0.5464	0.5172	0.5214	0.501	0.501	0.5185	0.5163
11	A_{49}-A_{52}	0.1	0.159	0.1	0.1	0.1	0.1004	0.1	0.1	0.1	0.1	0.1001
12	A_{53}-A_{54}	0.101	0.151	0.1	0.1	0.1095	0.1005	0.1007	0.1	0.1	0.104	0.1005
13	A_{55}-A_{58}	0.156	10.127	0.1	0.1	0.1615	0.1565	0.1566	0.16	0.168	0.1558	0.1563
14	A_{59}-A_{66}	0.547	7.32	0.525	0.524	0.5092	0.5507	0.5421	0.522	0.584	0.555	0.5448
15	A_{67}-A_{70}	0.442	3.812	0.394	0.4	0.4967	0.3922	0.4132	0.478	0.433	0.4052	0.4172
16	A_{71}-A_{72}	0.59	18.196	0.535	0.534	0.5619	0.5922	0.5756	0.591	0.52	0.567	0.5803
Weight (lb)		379.27	6818.67	369.65	369.65	381.91	379.85	379.66	381.03	380.62	379.834	379.643
Average weight (lb)		N/A	N/A	N/A	N/A	N/A	382.08	381.85	383.51	382.42	379.79	
Standard deviation (lb)		N/A	N/A	N/A	N/A	N/A	1.912	1.201	1.92	1.38	0.11	
Number of structural analyses		20,000	150,000	125,000	125,000	N/A	19, 621	13,200	15,044	13,742	14,275	13,499

Table 10. Optimization results obtained for Case 2 of the spatial 72-bar truss problem.

Design variables (A_i)	Element group	Area (in^2)								
		Lee and Geem [18]	Li et al. [22]			Lamberti [29]	Degertekin [21]		Present work	
		HS	PSO	PSOPC	HPSO	CMLPSA	EHS	SAHS	Worst result	Best result
1	A_1-A_4	1.963	40.053	1.652	1.907	1.8866	1.889	1.889	1.8892	1.9202
2	A_5-A_{12}	0.481	0.237	0.547	0.524	0.5169	0.502	0.52	0.5167	0.5112
3	A_{13}-A_{16}	0.01	21.692	0.1	0.01	0.01	0.01	0.01	0.01	0.01
4	A_{17}-A_{18}	0.011	0.657	0.101	0.01	0.01	0.01	0.01	0.01	0.01
5	A_{19}-A_{22}	1.233	22.144	1.102	1.288	1.2903	1.284	1.289	1.3668	1.3144
6	A_{23}-A_{30}	0.506	0.266	0.589	0.523	0.517	0.526	0.524	0.5125	0.5082
7	A_{31}-A_34	0.011	1.654	0.011	0.01	0.01	0.01	0.01	0.01	0.01
8	A_{35}-A_{36}	0.012	10.284	0.01	0.01	0.01	0.01	0.01	0.01	0.01
9	A_{37}-A_{40}	0.538	0.559	0.581	0.544	0.5207	0.528	0.539	0.5244	0.5252
10	A_{41}-A_{48}	0.533	12.883	0.458	0.528	0.518	0.525	0.519	0.5204	0.5209
11	A_{49}-A_{52}	0.01	0.138	0.01	0.019	0.01	0.01	0.015	0.0119	0.0102
12	A_{53}-A_{54}	0.167	0.188	0.152	0.02	0.1141	0.063	0.105	0.0553	0.116
13	A_{55}-A_{58}	0.161	29.048	0.161	0.176	0.1665	0.173	0.167	0.1734	0.1663
14	A_{59}-A_{66}	0.542	0.632	0.555	0.535	0.5363	0.55	0.532	0.5101	0.5341
15	A_{67}-A_{70}	0.478	3.045	0.514	0.426	0.446	0.444	0.425	0.4664	0.4503
16	A_{71}-A_{72}	0.551	1.711	0.648	0.612	0.5761	0.592	0.579	0.6496	0.5695
Weight (lb)		364.33	5417.02	368.45	364.86	363.818	364.36	364.05	364.4837	363.8838
Average weight (lb)		N/A	N/A	N/A	N/A	N/A	366.79	366.57	364.017	
Standard deviation (lb)		N/A	N/A	N/A	N/A	N/A	2.05	2.02	0.125	
Number of structural analyses		20,000	150,000	150,000	150, 000	900	13,755	12,852	12,935	12,298

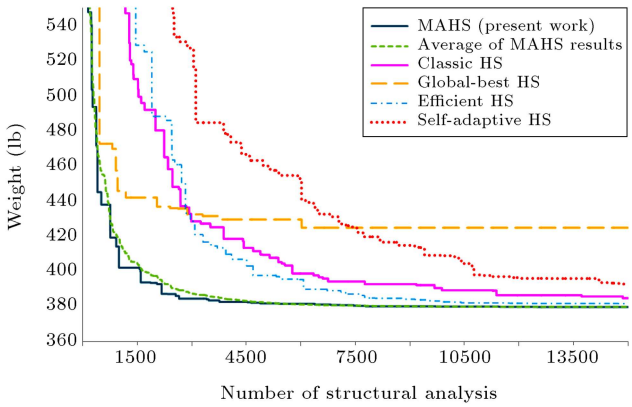

Figure 8. Comparison of HS variants convergence curves obtained for Case 1 of the spatial 72-bar truss problem.

Figure 8 for Case 1. It can be seen that the average converge history of MAHS is very close to that obtained for the best run. MAHS was always faster than HS variants that ranked in the same fashion as for the previous test problems.

5.1.4. Planar 200-bar truss

The fifth test problem is the weight minimization of the planar 200-bar truss shown in Figure 9. The modulus of elasticity of the material is 30 Msi while the material density is 0.283 lb/in^3. Element stresses must be less than 10,000 psi and no displacement constraints are considered. 200 members of truss are divided into 29 groups (see Table 11); therefore, this test problem consists of 29 sizing variables. The minimum cross-sectional area of all members was 0.1 in^2. The structure is subject to three independent loading conditions listed in Table 12.

Table 13 shows the optimum design found by MAHS and compares the present algorithm with literature. MAHS converged to the best feasible design with a small standard deviation. The worst result obtained in the 10 independent runs performed for this test problem was consistent with other designs quoted in literature. Classical HS obtained the optimum design after 48,000 analyses while MAHS required only 21,235 analyses.

Table 11. Design variables for the planar 200-bar truss.

Design variable	Member number
1	1, 2, 3, 4
2	5, 8, 11, 14, 17
3	19, 20, 21, 22, 23, 24
4	18, 25, 56, 63, 94, 101, 132, 139, 170, 177
5	26, 29, 32, 35, 38
6	6, 7, 9, 10, 12, 13, 15, 16, 27, 28, 30, 31, 33, 34, 36, 37
7	39, 40, 41, 42
8	43, 46, 49, 52, 55
9	57, 58, 59, 60, 61, 62
10	64, 67, 70, 73, 76
11	44, 45, 47, 48, 50, 51, 53, 54, 65, 66, 68, 69, 71, 72, 74, 75
12	77, 78, 79, 80
13	81, 84, 87, 90, 93
14	95, 96, 97, 98, 99, 100
15	102, 105, 108, 111, 114
16	82, 83, 85, 86, 88, 89, 91, 92, 103, 104, 106, 107, 109, 110, 112, 113
17	115, 116, 117, 118
18	119, 122, 125, 128, 131
19	133, 134, 135, 136, 137, 138
20	140, 143, 146, 149, 152
21	120, 121, 123, 124, 126, 127, 129, 130, 141, 142, 144, 145, 147, 148, 150, 151
22	153, 154, 155, 156
23	157, 160, 163, 166, 169
24	171, 172, 173,174, 175, 176
25	178, 181, 184, 187, 190
26	158, 159, 161, 162, 164, 165, 167, 168, 179, 180, 182, 183, 185, 186, 188, 189
27	191, 192, 193, 194
28	195, 197, 198, 200
29	196, 199

Table 12. Loading conditions for the planar 200-bar truss problem (kips).

Loading conditions	Nodes	Amount of load
Condition (1)	1, 6, 15, 20, 29,34, 43, 48, 57, 62 and 71	1 kips in positive X direction
Condition (2)	1, 2, 3, 4, 5, 6, 8, 10, 12, 14, 15, 16, 17, 18,19, 20, 22, 24, 26, 28,29 30, 31, 32, 33, 34, 36, 38, 40, 42, 43, 44, 45, 46, 47, 48, 50, 52, 54, 56, 57, 58, 59, 60, 61, 62, 64, 66, 68, 70, 71, 72, 73, 74 and 75	10 kips in negative Y direction
Condition (3)	Loading conditions (1) and (2) acting together.	

The convergence curves, shown in Figure 10, prove that the average optimization history of MAHS is very close to that found for the best run. The present algorithm is definitely superior over other HS variants which ranked in the same order as in the previous examples.

Figure 11 shows the existing and allowable element stress values for the loading conditions 1, 2 and 3, respectively.

5.2. Frame structures

5.2.1. Planar ten-story one-bay planar frame

The first frame design problem solved in this study is the weight minimization of the one-bay ten-story

Table 13. Optimization results obtained for the planar 200-bar truss problem.

Design variables (A_i)	Area (in^2)								
	Lee and Geem [18]	Lamberti [29]	Kaveh and Talatahari [23]			Degertekin [21]		Present work	
	HS	CMLPSA	PSO	PSOPC	HPSOACO	EHS	SAHS	Worst result	Best result
1	0.1253	0.1468	0.8016	0.759	0.1033	0.15	0.154	0.1370	0.1411
2	1.0157	0.94	2.4028	0.9032	0.9184	0.946	0.941	1.0564	0.9775
3	0.1069	0.1	4.3407	1.1	0.1202	0.101	0.1	0.1001	0.1113
4	0.1096	0.1	5.6972	0.9952	0.1009	0.1	0.1	0.1001	0.1001
5	1.9369	1.94	3.9538	2.135	1.8664	1.945	1.942	1.9534	1.9451
6	0.2686	0.2962	0.595	0.4193	0.2826	0.296	0.301	0.2881	0.2969
7	0.1042	0.1	5.608	1.0041	0.1	0.1	0.1	0.1015	0.1006
8	2.9731	3.1042	9.1953	2.8052	2.9683	3.161	3.108	3.1136	3.1149
9	0.1309	0.1	4.5128	1.0344	0.1	0.102	0.1	0.1106	0.1003
10	4.1831	4.1042	4.6012	3.7842	3.9456	4.199	4.106	4.1136	4.118
11	0.3967	0.4034	0.5552	0.5269	0.3742	0.401	0.409	0.4162	0.4078
12	0.4416	0.1912	18.751	0.4302	0.4501	0.181	0.191	0.1472	0.1425
13	5.1873	5.4284	5.9937	5.2683	4.9603	5.431	5.428	5.4349	5.4325
14	0.1912	0.1	0.1	0.9685	1.0738	0.1	0.1	0.1327	0.1504
15	6.241	6.4284	8.1561	6.0473	5.9785	6.428	6.427	6.4348	6.4224
16	0.6994	0.5734	0.2712	0.7825	0.7863	0.571	0.581	0.5807	0.5782
17	0.1158	0.1327	11.152	0.592	0.7374	0.156	0.151	0.2574	0.1691
18	7.7643	7.9717	7.1263	8.1858	7.3809	7.961	7.973	7.9871	7.9777
19	0.1	0.1	4.465	1.0362	0.6674	0.1	0.1	0.2851	0.1001
20	8.8279	8.9717	9.1643	9.2062	8.3	8.959	8.974	8.9867	8.9792
21	0.6986	0.7049	2.7617	1.4774	1.1967	0.722	0.719	0.9214	0.7423
22	1.5563	0.4196	0.5541	1.8336	1.0	0.491	0.422	0.6071	0.4615
23	10.9806	10.8636	16.164	10.611	10.8262	10.909	10.892	11.3988	10.9658
24	0.1317	0.1	0.4974	0.9851	0.1	0.101	0.1	0.1828	0.1002
25	12.1492	11.8606	16.225	12.509	11.6976	11.985	11.887	12.4178	11.9658
26	1.6373	1.0339	1.0042	1.9755	1.388	1.084	1.04	1.3514	1.0849
27	5.0032	6.6818	3.6098	4.5149	4.9523	6.464	6.646	5.2179	6.2849
28	9.3545	10.8113	8.3684	9.8	8.8	10.802	10.804	9.9046	10.7115
29	15.0919	13.8404	15.562	14.531	14.6645	13.936	13.87	14.7564	13.9967
Weight (lb)	25447.1	25445.63	44081.4	28537.8	25156.5	25542.5	25491.9	25650	25482.21
Average weight (lb)	N/A	N/A	N/A	N/A	N/A	25659.71	25610.2	25545.11	
Standard deviation (lb)	N/A	N/A	N/A	N/A	N/A	164.17	148.85	49.69	
Number of structural analyses	48,000	9,650	150,000	150,000	9,875	22,851	19,670	22,425	21,235

frame shown in Figure 12. The modulus of elasticity is 29 Msi while yield stress is 36 ksi. The frame includes 30 members connected by 22 joints. Because of structural symmetry, elements are grouped in 5 groups of columns and 4 groups of beams (see Figure 12). This test problem included discrete optimization variables. Cross-sectional areas of beam elements can be selected from 267 W-sections, while cross-sectional areas of columns can be selected from $W14$ and $W12$ sections.

The frame was previously optimized by Pezeshk et al. [30] using GA and by Camp et al. [31] using ACO. The effective length factors of members were

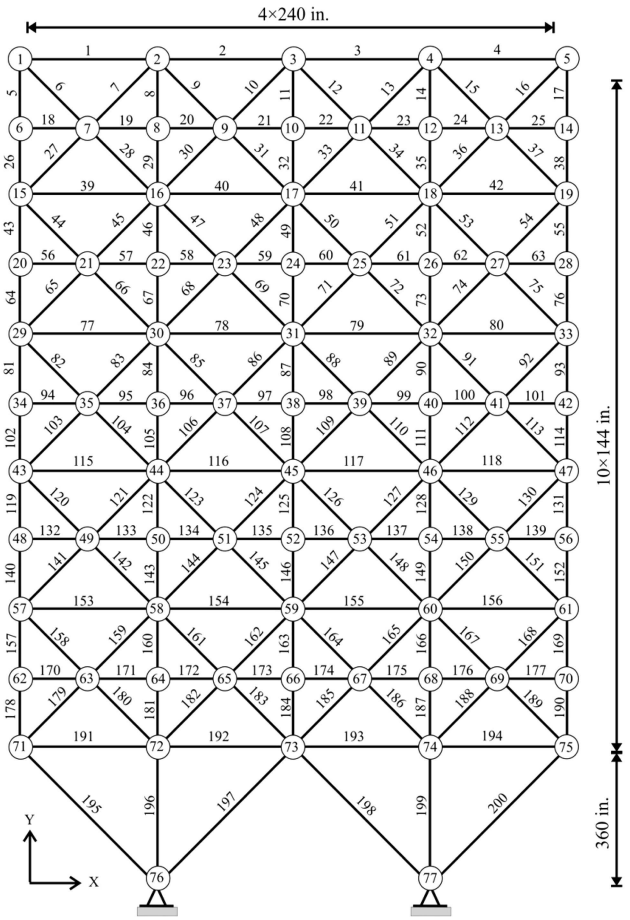

Figure 9. Schematic of planar 200-bar truss [21].

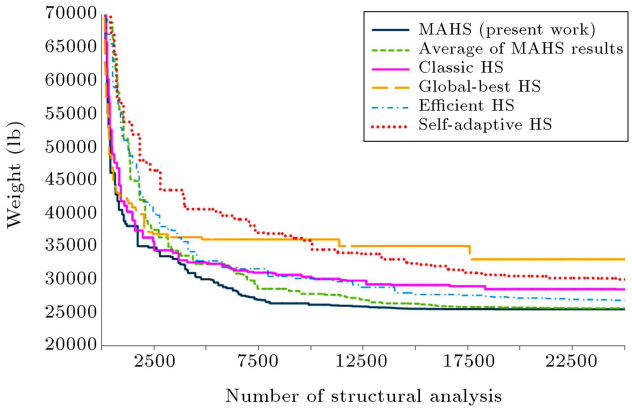

Figure 10. Comparison of HS variants convergence curves obtained for the planar 200-bar truss problem.

calculated as $K_x \geq 1$ for sway-permitted frame using the approximate equation developed by Dumonteil [32], whereas the out-of-plane length factor is $K_y = 1$. For each beam member, the out-of-plane effective length factor was set as $K_y = 0.2$.

Table 14 compares the optimum design found by MAHS with literature. It can be seen that the present algorithm converged to a feasible design weighing 63,322 lb which is 2.78% lighter than the

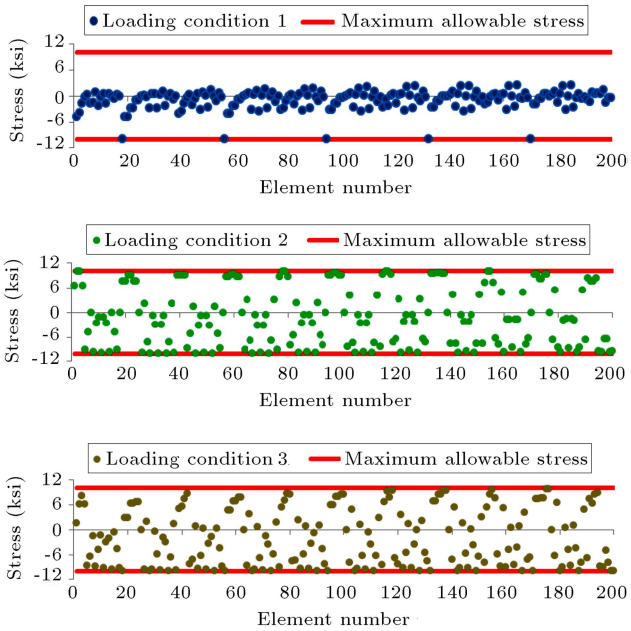

Figure 11. Comparison of the allowable and existing element stresses for the planar 200-bar truss problem using the MAHS.

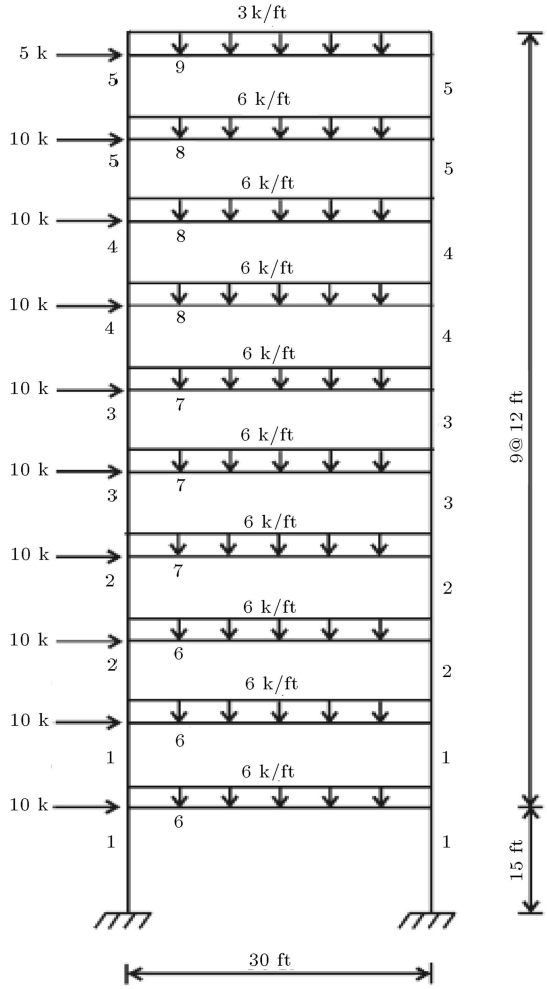

Figure 12. Ten-story one-bay frame [33].

Table 14. Optimization results obtained for the ten-story one-bay frame problem.

Design variables		Section				
		Pezeshk et al. [30]	Camp et al. [31]	Degertekin [33]	Present work	
		GA	ACO	HS	Worst result	Best result
Columns	1	$W14 \times 233$	$W14 \times 233$	$W14 \times 211$	$W14 \times 233$	$W14 \times 233$
	2	$W14 \times 176$	$W14 \times 176$	$W14 \times 176$	$W14 \times 176$	$W14 \times 176$
	3	$W14 \times 159$	$W14 \times 145$	$W14 \times 145$	$W14 \times 159$	$W14 \times 159$
	4	$W14 \times 99$	$W14 \times 99$	$W14 \times 90$	$W14 \times 99$	$W14 \times 99$
	5	$W12 \times 79$	$W12 \times 65$	$W14 \times 61$	$W12 \times 65$	$W12 \times 65$
Beams	6	$W33 \times 118$	$W30 \times 108$	$W33 \times 118$	$W36 \times 135$	$W33 \times 118$
	7	$W30 \times 90$	$W30 \times 90$	$W30 \times 99$	$W30 \times 99$	$W30 \times 90$
	8	$W27 \times 84$	$W27 \times 84$	$W24 \times 76$	$W27 \times 84$	$W27 \times 84$
	9	$W24 \times 55$	$W21 \times 44$	$W18 \times 46$	$W21 \times 55$	$W21 \times 55$
Weight (lb)		65,136	62,610	61,864	64,390	63,322
Average weight (lb)		N/A	N/A	62923	64129	
Standard deviation (lb)		N/A	N/A	1.74	219	
Number of structural analyses		3,000	8,300	3,690	2,555	1,095

optimum design found by GA [30]. Furthermore, the standard deviation of 20 different runs was very small: only 219 lb. GA [30], ACO [31] and classical HS [33] completed the optimization process within, respectively, 3000, 8300 and 3690 structural analyses while MAHS required only 1095 structural analyses.

The number of structural analyses required in the worst optimization run is higher than that required in the best optimization run. A possible reason for such a behavior is in the discrete nature of the frame problems.

Convergence curves of HS variants are compared in Figure 13 for a maximum number of structural analyses set as 3,500 for all algorithms. Sensitivity analysis was performed for all HS variants and 20 independent optimization runs were then conducted starting from different initial designs. It can be seen that the average convergence curve of MAHS is very close to that obtained for the best optimization run. The present algorithm was the fastest HS variant followed by SAHS.

In Figure 14, inter-story drift for each story is de-

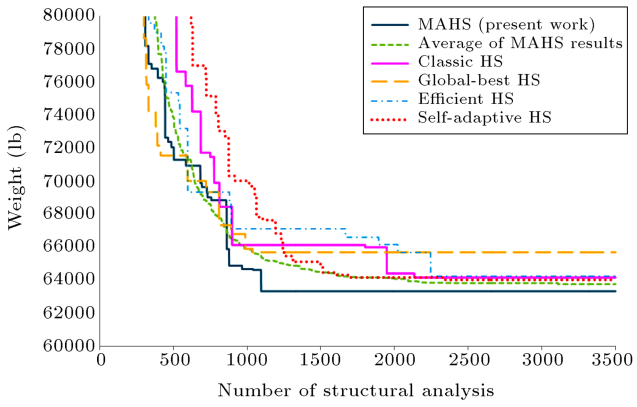

Figure 13. Comparison of HS variants convergence curves obtained for the ten-story one-bay frame problem.

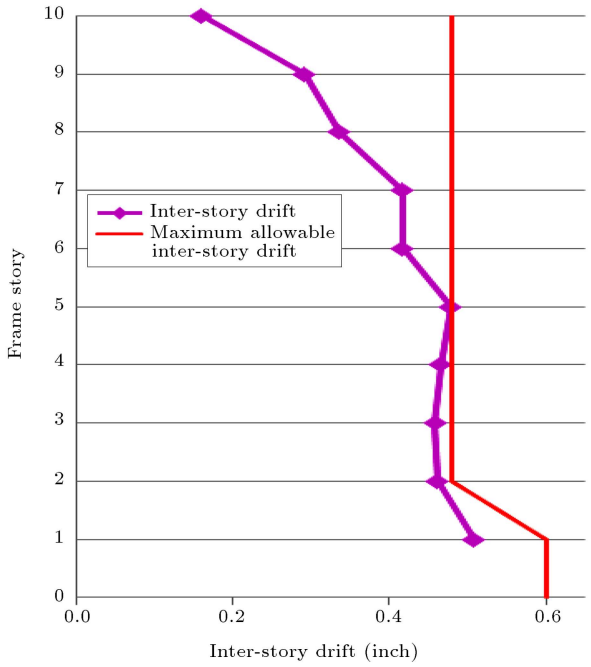

Figure 14. Comparison of the allowable and existing inter-story drift for the ten-story one-bay frame problem using the MAHS.

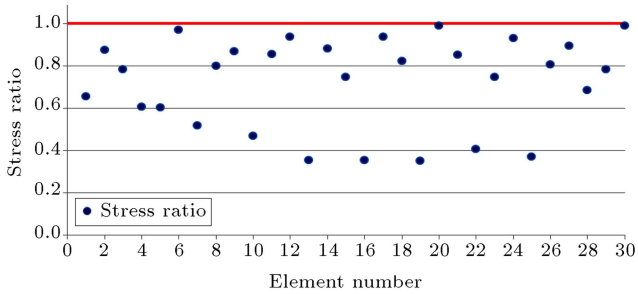

Figure 15. Comparison of the allowable and existing element stresses for the ten-story one-bay frame problem using the MAHS.

picted and compared to the allowable drift value. The maximum inter-story drift evaluated for the optimized design was 99.5% of the allowable value at the fifth story. The global sway at the top story was 3.98 in, less than the maximum permitted sway (4.92 in). Element stresses also were smaller than the corresponding limit shown in Figure 15.

5.2.2. Planar twenty four-story three-bay frame

The second test case with discrete variables was the weight minimization of the 3-bay 24-story frame shown in Figure 16. The frame included 100 joints connected by 168 elements. The modulus of elasticity of the material is $E = 29,732$ ksi (205 GPa) and the yield stress is $f_y = 33,400$ psi (230.3 MPa). The columns in a story are grouped in two groups of exterior columns and interior columns. Furthermore, columns belonging to three adjacent stories are grouped together. The beams of each story are divided into two groups as beam of inner bay and beams of outer bays. Beams are grouped together for all stories except the roof. Therefore, the 168 frame elements can be divided in 20 groups and the optimization problem includes 20 sizing variables. Cross-sectional areas of the 4 groups of beams can be selected from all 267 W-sections, while cross-sectional areas of the 16 groups of columns can be selected only from $W14$ sections (37 W-shapes). The frame is subjected to the loads listed in Table 15. The structure is designed according the AISC-LRFD specifications [19] with an inter-story drift displacement constraint. The effective length factors of the members are calculated as $K_x \geq 0$ for a sway-permitted frame using the approximate equation proposed by Dumonteil [32]. The out-of-plane effective length factor is specified as $K_y = 1.0$. All columns and beams are considered as non-braced along their lengths.

Table 16 compares the MAHS optimum design with literature. The proposed algorithm converged to the best design without violating optimization constraints. The worst design obtained in the 10 independent optimization runs carried out from different initial populations is better than the other designs reported in

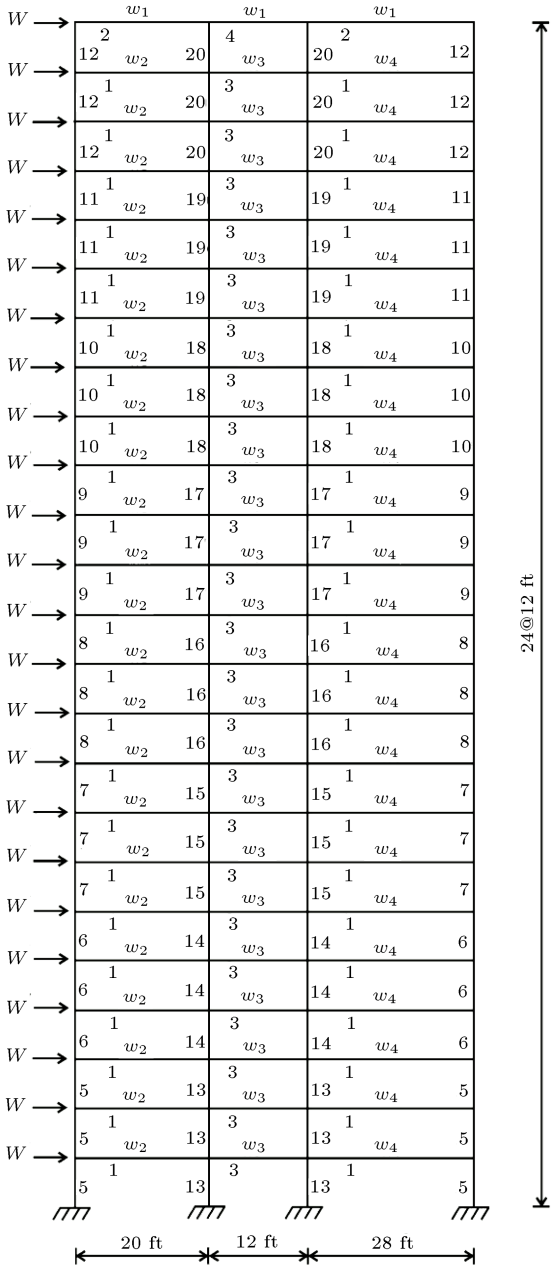

Figure 16. Schematic of the twenty four-story three-bay frame [33].

literature. The standard deviation on optimized weight was only 1320 lb, smaller than for CSS. The MAHS algorithm required only 7115 structural analyses, hence less than ACO [31], HS [33] and ICA [35].

Optimization histories of HS variants are compared in Figure 17 for a maximum number of structural analyses equal to 14,000. Sensitivity analysis was carried out for each HS algorithm to find the best combination of internal parameters, and 10 independent optimization runs were carried out starting from different initial populations. The convergence curves relative to the best optimization run are shown for each HS variant. Remarkably, the average convergence

curve of MAHS was better than the best convergence curves obtained for the other HS variants.

The optimized design fully satisfied the optimization constraints. Figure 18 shows the inter-story drift for each story and compares to the allowable drift value.

Table 15. Loading conditions for the twenty four-story three-bay frame problem.

Type			Amount
W	Lateral	Left joints	5761.85 (lb)
w_1	Gravity	Roof beams	300 (lb/ft)
w_2		Left outer beams	436 (lb/ft)
w_3		Inner beams	474 (lb/ft)
w_4		Right outer beams	408 (lb/ft)

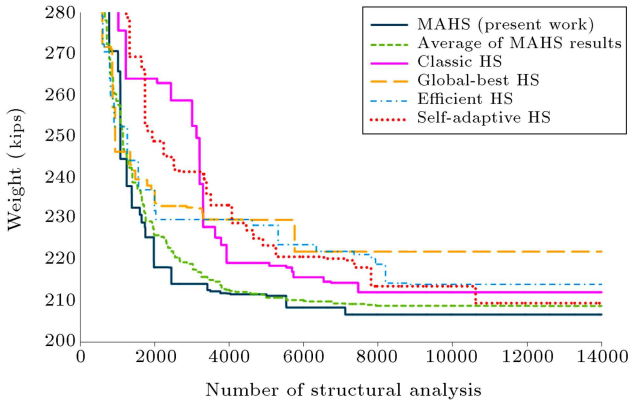

Figure 17. Comparison of HS variants convergence curves obtained for the twenty four-story three-bay frame problem.

Table 16. Optimization results obtained for the twenty four-story three-bay frame problem.

	Design variables	Section						
		Camp et al. [31]	Degertekin [33]	Kaveh and Talatahari			Present work	
		ACO	HS	IACO [34]	ICA [35]	CSS [36]	Worst result	Best result
Beams	1	$W30 \times 90$	$W30 \times 90$	$W30 \times 99$	$W30 \times 90$	$W30 \times 90$	$W30 \times 90$	$W30 \times 90$
	2	$W8 \times 18$	$W10 \times 22$	$W16 \times 26$	$W21 \times 50$	$W21 \times 50$	$W12 \times 68$	$W10 \times 49$
	3	$W24 \times 55$	$W18 \times 40$	$W18 \times 35$	$W24 \times 55$	$W21 \times 48$	$W24 \times 44$	$W21 \times 48$
	4	$W8 \times 21$	$W12 \times 16$	$W14 \times 22$	$W8 \times 28$	$W12 \times 19$	$W14 \times 19$	$W12 \times 40$
Columns	5	$W14 \times 145$	$W14 \times 176$	$W14 \times 145$	$W14 \times 109$	$W14 \times 176$	$W14 \times 233$	$W14 \times 176$
	6	$W14 \times 132$	$W14 \times 176$	$W14 \times 132$	$W14 \times 159$	$W14 \times 145$	$W14 \times 145$	$W14 \times 145$
	7	$W14 \times 132$	$W14 \times 132$	$W14 \times 120$	$W14 \times 120$	$W14 \times 109$	$W14 \times 109$	$W14 \times 109$
	8	$W14 \times 132$	$W14 \times 109$	$W14 \times 109$	$W14 \times 90$	$W14 \times 90$	$W14 \times 61$	$W14 \times 74$
	9	$W14 \times 68$	$W14 \times 82$	$W14 \times 48$	$W14 \times 74$	$W14 \times 74$	$W14 \times 53$	$W14 \times 61$
	10	$W14 \times 53$	$W14 \times 74$	$W14 \times 48$	$W14 \times 68$	$W14 \times 61$	$W14 \times 53$	$W14 \times 61$
	11	$W14 \times 43$	$W14 \times 34$	$W14 \times 34$	$W14 \times 30$	$W14 \times 34$	$W14 \times 30$	$W14 \times 30$
	12	$W14 \times 43$	$W14 \times 22$	$W14 \times 30$	$W14 \times 38$	$W14 \times 34$	$W14 \times 22$	$W14 \times 22$
	13	$W14 \times 145$	$W14 \times 145$	$W14 \times 159$	$W14 \times 159$	$W14 \times 145$	$W14 \times 90$	$W14 \times 99$
	14	$W14 \times 145$	$W14 \times 132$	$W14 \times 120$	$W14 \times 132$	$W14 \times 132$	$W14 \times 99$	$W14 \times 109$
	15	$W14 \times 120$	$W14 \times 109$	$W14 \times 109$	$W14 \times 99$	$W14 \times 109$	$W14 \times 109$	$W14 \times 99$
	16	$W14 \times 90$	$W14 \times 82$	$W14 \times 99$	$W14 \times 82$	$W14 \times 82$	$W14 \times 120$	$W14 \times 90$
	17	$W14 \times 90$	$W14 \times 61$	$W14 \times 82$	$W14 \times 68$	$W14 \times 68$	$W14 \times 90$	$W14 \times 74$
	18	$W14 \times 61$	$W14 \times 48$	$W14 \times 53$	$W14 \times 48$	$W14 \times 43$	$W14 \times 53$	$W14 \times 53$
	19	$W14 \times 30$	$W14 \times 30$	$W14 \times 38$	$W14 \times 34$	$W14 \times 34$	$W14 \times 43$	$W14 \times 34$
	20	$W14 \times 26$	$W14 \times 22$	$W14 \times 26$	$W14 \times 22$	$W14 \times 22$	$W14 \times 26$	$W14 \times 26$
Weight (lb)		220,465	214,860	217,475	212,735	212,459	211,172.9	206,224.9
Average weight (lb)		229,552	222,620	N/A	N/A	215,313	208,776	
Standard deviation (lb)		4561	5800	N/A	N/A	2448	1320	
Number of structural analyses		15,500	13,924	3500	7,500	5,500	10,918	7,115

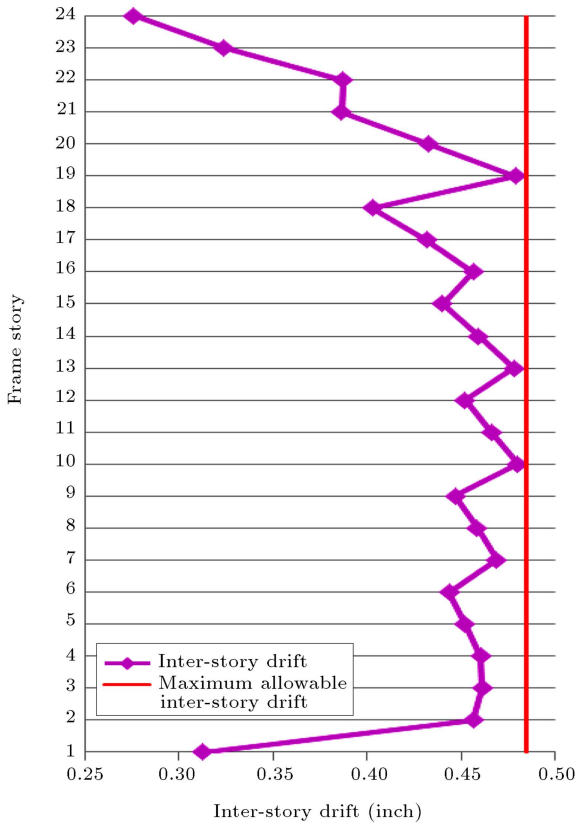

Figure 18. Comparison of the allowable and existing inter-story drift for the twenty four-story three-bay frame problem using the MAHS.

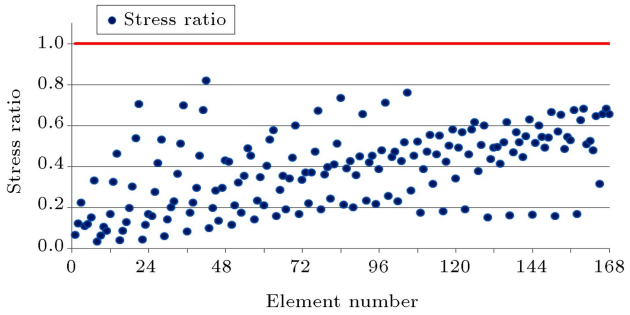

Figure 19. Comparison of the allowable and existing element stresses for the twenty four-story three-bay frame problem using the MAHS.

The global sway at the top story was 10.31 in, less than the maximum permitted sway (11.52 in).

In Figure 19, the existing and allowable element stresses for each member are shown. Inter-story drift governed the design process while stress constraints were less critical.

6. Concluding remarks

This study presented an improved Harmony Search algorithm termed as Multi-Adaptive Harmony Search (MAHS). The internal parameters of MAHS are adaptively modified to improve robustness and convergence behavior with respect to classical HS and other HS variants recently published in literature.

The new proposed algorithm was successfully utilized in sizing optimization problems of truss and frame structures with continuous and discrete design variables. The new mechanism of pitch-adjusting introduced in MAHS leads to obtain better results and faster convergence because the diversification and intensification stages of the optimization search process are very well balanced. Consequently, the computational cost of MAHS is considerably smaller than other HS variants. Furthermore, the standard deviation of optimized weight over independent runs carried out starting from different initial populations is very small.

Acknowledgments

The first author is grateful to the Iran National Science Foundation for the support.

References

1. Osman, I.H. and Laporte, G. "Metaheuristics: A bibliography", *Annals of Operations Research*, **63**(5), pp. 513-623 (1996).
2. Holland, J.H., *Adaptation in Natural and Artificial Systems*, MIT Press Cambridge, MA, USA (1992).
3. Goldberg, D.E., *Genetic Algorithms in Search Optimization and Machine Learning*, Addison-Wesley, Boston, MA, USA (1989).
4. Glover, F. "Heuristic for integer programming using surrogate constraints", *Decision Sciences*, **8**(1), pp. 156-166 (1977).
5. Dorigo, M., Maniezzo, V. and Colorni A. "The ant system: Optimization by a colony of cooperating agents", *IEEE Transactions on Systems, Man, and Cybernetics, Part B*, **26**(1), pp. 29-41 (1996).
6. Eberhart, R.C. and Kennedy, J. "A new optimizer using particle swarm theory", In: *Proceedings of the Sixth International Symposium on Micro Machine and Human Science*, Nagoya, Japan, IEEE Press, Piscataway, NJ, pp. 39-43 (1995).
7. Kirkpatrick, S., Gelatt, C.D. and Vecchi, M.P. "Optimization by simulated annealing", *Science*, **220**(4598), pp. 671-680 (1983).
8. Erol, O.K. and Eksin, I. "New optimization method: Big bang-big crunch", *Advances in Engineering Software*, **37**(2), pp. 106-111 (2006).
9. Kaveh, A. and Talatahari, S. "A novel heuristic optimization method: Charged system search", *Acta Mechanica*, **213**(3-4), pp. 267-289 (2010).
10. Geem, Z.W., Kim, J.H. and Loganathan, G.V. "A new heuristic optimization algorithm: Harmony search", *Simulation*, **76**(2), pp. 60-68 (2001).

11. Geem, Z.W. "State-of-the-art in the structure of harmony search algorithm", in: *Recent Advances in Harmony Search Algorithm, Studies in Computational Intelligence*, **270**, pp. 1-10 (2010).
12. Mahdavi, M., Fesanghary, M. and Damangir, E. "An improved harmony search algorithm for solving optimization problems", *Applied Mathematics and Computation*, **188**(2), pp. 1567-1579 (2007).
13. Geem, Z.W. "Novel derivative of harmony search algorithm for discrete design variables", *Applied Mathematics and Computation*, **199**(1), pp. 223-230 (2008).
14. Omran, M.G.H. and Mahdavi, M. "Global-best harmony search", *Applied Mathematics and Computation*, **198**(2), pp. 643-656 (2008).
15. Wang, C.M. and Huang, Y.F. "Self-adaptive harmony search algorithm for optimization", *Expert Systems with Applications*, **37**(4), pp. 2826-2837 (2010).
16. Fesanghary, M., Mahdavi, M., Minary-Jolandan, M. and Alizadeh, Y. "Hybridizing harmony search algorithm with sequential quadratic programming for engineering optimization problems", *Computer Methods in Applied Mechanics and Engineering*, **197**(33-40), pp. 3080-3091 (2008).
17. Saka, M.P. and Hasancebi, O. "Adaptive harmony search algorithm for design code optimization of steel structures, harmony search algorithms for structural design optimization", In: *Studies in Computational Intelligence*, Geem, Z.W, Ed., **239**, Berlin, Heidelberg: Springer-Verlag, pp. 79-120 (2009).
18. Lee, K.S. and Geem, Z.W. "A new structural optimization method based on the harmony search algorithm", *Computers and Structures*, **82**(9-10), pp. 781-798 (2004).
19. American Institute of Steel Construction (AISC), *Manual of Steel Construction-Load Resistance Factor Design*, 2nd Ed, Chicago, AISC (1992).
20. Kaveh, A., Farahmand Azar, B. and Talatahari, S. "Ant colony optimization for design of space trusses", *International Journal of Space Structures*, **23**(3), pp. 167-81 (2008).
21. Degertekin, S.O. "Improved harmony search algorithms for sizing optimization of truss structures", *Computers and Structures*, **92-93**, pp. 229-241 (2012).
22. Li, L.J., Huang, Z.B., Liu, F. and Wu, Q.H. "A heuristic particle swarm optimizer for optimization of pin connected structures", *Computers and Structures*, **85**(7-8), pp. 340-349 (2007).
23. Kaveh, A. and Talatahari, S. "Particle swarm optimizer, ant colony strategy and harmony search scheme hybridized for optimization of truss structures", *Computers and Structures*, **87**(5-6), pp. 267-283 (2009).
24. Lamberti, L. and Pappalettere, C. "An improved harmony-search algorithm for truss structure optimization", In: *Proceedings of the Twelfth International Conference Civil, Structural and Environmental Engineering Computing*, Topping, B.H.V., Neves, L.F.C. and Barros, R.C., Eds., Stirlingshire, Scotland: Civil-Comp Press (2009).
25. Schmit Jr, L.A. and Farshi, B. "Some approximation concepts for structural synthesis", *American Institute of Aeronautics and Astronautics Journal*, **12**(5), pp. 692-699 (1974).
26. Perez, R.E. and Behdinan, K. "Particle swarm approach for structural design optimization", *Computers and Structures*, **85**(19-20), pp.1579-1588 (2007).
27. Camp, C.V. "Design of space trusses using big bang-big crunch optimization", *Journal of Structural Engineering (ASCE)*, **133**(7), pp. 999-1008 (2007).
28. Kaveh, A. and Talatahari, S. "Size optimization of space trusses using big-bang big-crunch algorithm", *Computers and Structures*, **87**(17-18), pp. 1129-1140 (2009).
29. Lamberti, L. "An efficient simulated annealing algorithm for design optimization of truss structures", *Computers and Structures*, **86**(19-20), pp. 1936-1953 (2008).
30. Pezeshk, S., Camp C.V. and Chen, D. "Design of nonlinear framed structures using genetic optimization", *Journal of Structural Engineering (ASCE)*, **126**, pp. 382-388 (2000).
31. Camp, C.V., Bichon, B.J. and Stovall, S.P. "Design of steel frames using ant colony optimization", *Journal of Structural Engineering (ASCE)*, **131**, pp. 369-379 (2005).
32. Dumonteil, P. "Simple equations for effective length factors", *Journal of Structural Engineering (ASCE)*, **3**, pp. 111-115 (1992).
33. Degertekin, S.O. "Optimum design of steel frames using harmony search algorithm", *Structural and Multidisciplinary Optimization*, **36**(4), pp. 393-401 (2008).
34. Kaveh, A. and Talatahari, S. "An improved ant colony optimization for design of planar steel frames", *Engineering Structures*, **32**(3), pp. 864-876 (2010).
35. Kaveh, A. and Talatahari, S. "Optimum design of skeletal structures using imperialist competitive algorithm", *Computers and Structures*, **88**(21-22), pp. 1220-1229 (2010).
36. Kaveh, A. and Talatahari, S. "Charged system search for optimal design of frame structures", *Applied Soft Computing*, **12**(1), pp. 382-393 (2012).

Biographies

Ali Kaveh was born in 1948 in Tabriz, Iran. After graduation from the Department of Civil Engineering at the University of Tabriz in 1969, he continued his studies on Structures at Imperial College of Science and Technology at London University, and received his MS, DIC and PhD degrees in 1970 and 1974, respectively. He then joined the Iran University of Science and Technology in Tehran where he is presently Professor of Structural Engineering. Professor Kaveh is the author of 420 papers published in international journals and 135 papers presented at international

conferences. He has authored 23 books in Farsi and 7 books in English published by Wiley, the American Mechanical Society, Research Studies Press and Springer-Verlag.

Mohammad Naeimi was born in 1986 in Tehran, Iran. He obtained his BS degree in Civil Engineering from Khajeh Nasir Toosi University of Technology (KNTU) in 2010, and received his MS degree in Earthquake Engineering from Road, Housing and Urban Development Research Centre in 2013. At present, he studies on optimal design of structures with frequency constraints. His main research interests include: Structural optimization, topology optimization, structural dynamics, seismic fragility of structural systems and soil-structure interaction.